



# The Solar System as a Benchmark for Exoplanet Systems Interpretation

# 20

Pilar Montañés-Rodríguez and Enric Pallé

## Contents

Introduction	422
The Solar System Planets: A Subsample Within the Planetary Zoo	423
Characterization of Planetary Atmospheres	424
Solar System Planets in Reflected Light	425
Reflected Light of Earth and Earthshine	426
Transmission Spectroscopy and Solar System	429
Transit of Mercury	430
Transit of Venus	430
Transit of the Earth	431
Transit of Mars	433
Transit of Jupiter	435
Transit of Saturn	435
Transit of Titan	436
Transits of Uranus and Neptune	437
Concluding Remarks	438
References	438

## Abstract

For hundreds of years, the Solar System and its planetary bodies were the only example in which to base our models of planet formation and evolution. With the discovery of exoplanets, a much greater diversity of planetary types and system architectures have been uncovered. Nevertheless, the Solar System planets remain our best test bed to understand planetary physics and interpret low signal-to-noise exoplanetary observations. Here, we put the Solar System planets in context to the broader planetary population in our galaxy and detail

---

P. Montañés-Rodríguez (✉) · E. Pallé  
Instituto de Astrofísica de Canarias, La Laguna, Tenerife, Spain  
e-mail: [pmr@iac.es](mailto:pmr@iac.es); [epalle@iac.es](mailto:epalle@iac.es)

the several observations of our Solar System planets that have been performed with the goal of observing them as exoplanets. We pay special attention to the only planet known to host life in our galaxy so far, the Earth.

---

## Introduction

The Solar System can be described as constituted by eight planets and several dwarf planets, all of them gravitationally bound to a main sequence G2V star 4.5–4.6 Gyr old (Armitage 2010). Besides planets and satellites, the Solar System also possesses the main asteroid belt (which contains several dwarf planets) located between the orbits of Mars and Jupiter; the trans-Neptunian, or Kuiper belt, beyond the orbit of Neptune; and the Oort Cloud, a spherical shell surrounding the Sun and formed by icy objects (see also ► [Chap. 19, “The Diverse Population of Small Bodies of the Solar System”](#) by de Leon et al., on this handbook).

The four interior planets are small and rocky with  $R_P = 0.4 - 1.0 R_E$ , and the four longer period larger planets have radius ranging  $0.4 - 1.0 R_J$ . Practically all their orbits are circular, with their eccentricities ranging from 0.068 to 0.21. The alignment of the orbits is also significant, with the individual inclinations ranging from  $0^\circ.33$  to  $6^\circ.3$  relative to the plane defined by the total angular momentum of the system. The star’s equator is tilted by  $6^\circ$  relative to this plane, whereas its rotational angular momentum is quite smaller than the orbital angular momentum of the planets (Winn and Fabrycky 2015).

These facts are essential to describe the formation model for our Solar System, but it is still unknown whether all planetary systems form and evolve in the same way, or if several paths are possible. In this sense, the understanding of the Solar System dynamics (Fernandez and Ip 1984; Ip and Fernandez 1988; Malhotra 1995) has been an important achievement allowing the approach toward exoplanetary systems. The *Nice* model of Solar System formation succeeds on reproducing much of the observed orbital architecture of the Solar System (Gomes et al. 2005; Morbidelli et al. 2005; Tsiganis et al. 2005).

The role played by planetary migration (Armitage 2007; Kley and Nelson 2012) has been very important, in particular the migration of the giant planets with the Grand Tack model (Walsh et al. 2011, 2012; Morbidelli et al. 2012).

Understanding planetary systems formation and evolution is one of the major areas of exoplanet research, and to solve it requires both theoretical simulations and empirical observations. In this sense, our understanding of the Solar System, which has changed substantially over the last years, plays a fundamental role in understanding other planets.

In this paper, we briefly describe how the Solar System fits in the current scenario of the discovered exoplanetary systems. We later review the observations of different Solar System planets, as if they were observed from an astronomical distance.

## The Solar System Planets: A Subsample Within the Planetary Zoo

The variety of Solar System bodies constitutes a benchmark to address the study of extraSolar Systems, and on the other hand, the observation of protoplanetary disks and exoplanets is contributing to our understanding of Solar System formation (Wright 2010; Deming and Seager 2009; Wyatt 2008; Chambers 2016; Alessi et al. 2017).

But how similar is the exoplanet population to that of the Solar System? Is there a much broader variety of planet architecture and physical properties?

The first exoplanets discovered was 51 Peg b (Mayor and Queloz 1995), a planet with half a Jupiter mass orbits a star at a distance six times closer than the radius of Mercury's orbit. These are the so-called hot Jupiters, for which we have now many examples, which are a consequence of planet migration through protoplanetary disk and stochastic planet formation (Lin et al. 1996), although some recent studies have also considered the possibility of in situ formation through core accretion (Lee et al. 2014; Boley et al. 2016; Batygin et al. 2016). Several giant planets have quite eccentric orbits, HD80606b, for example, (Laughlin et al. 2009) reaches  $e=0.93$ . This planet receives at periastron a radiation from the star which varies substantially, between 10,000 and 10 times the flux received by the Earth from the Sun, at periastron and apastron, respectively.

Figure 1 shows planet mass and orbital period for the confirmed exoplanets using different detection techniques. From the figure we can summarize that, for orbital periods shorter than a few years, companions with estimated masses between 10 and 100  $M_J$  (planet radius between 1 and 2  $R_J$ ) are less frequent at orbital periods shorter than a few years than less massive planets. This figure provides a good overview, but it does not have into account the selection effects. Giant planets dominate the observed distribution, but occurrence rates can be quantified via numerical simulation (see Burke 2015 for instance), which show how small planets are frequent and close-in giants are much less abundant (Winn and Fabrycky 2015; Batalha 2014). This seems to be particularly true for small M-type stars, as a large fraction of these objects are hosts to low-mass, multi-planetary systems. In fact, it appears that the occurrence rates of planets around nearby M-dwarfs could be as high as 100% (Bonfils et al. 2013; Tuomi and Anglada-Escudé 2013; Tuomi et al. 2014), with the fraction of habitable zone planets reaching up to 20%. These results are in agreement with photometric analysis of fainter M-dwarfs using data from the Kepler satellite (Dressing and Charbonneau 2013).

Exoplanets with masses between 0.03 and 1  $M_J$  are known as Neptunes (Neptune's mass is 17 Earth masses), whereas planets between the size of the Earth and Neptune are called sub-Neptunes. Approximately 30% of Sun-like stars host sub-Neptunes with orbital periods  $P < 100$  days (Howard et al. 2012, Burke 2015). Hot Neptunes (orbit radius  $< 0.5$  AU) comprise 13% of all known exoplanets and warm Neptunes ( $0.5 < \text{orbit radius} < 2$  AU) are 1.5%. But no exoplanets are known to be as far out from their host stars as Uranus and Neptune are from the Sun

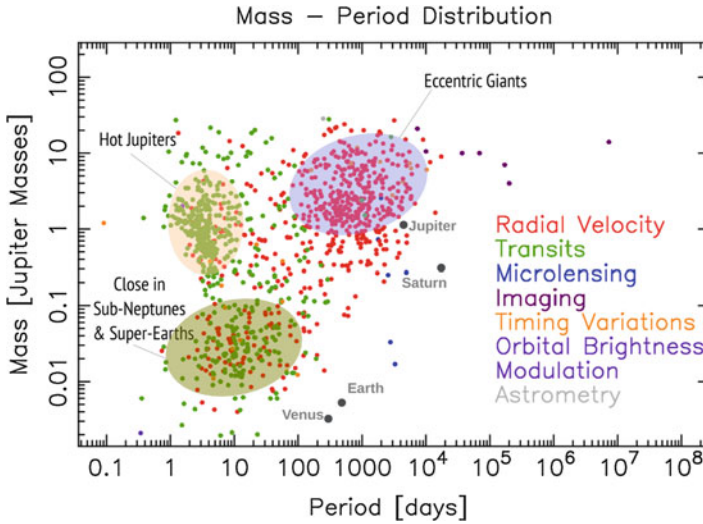


**Fig. 1** Mass – orbital period relationship of confirmed exoplanets based on a March 2017 query of the NASA exoplanet archive. They have been detected by different techniques; for transiting planets, thousands of candidates identified by the Kepler mission are missing. For radial velocity planets, the plotted mass is really  $M_p \sin i$ . For imaging planets, the mass is based on theoretical models relating the planets’s age, luminosity, and mass. For microlensing planets, the planet mass is determined from the planet-to-star mass ratio. For both, microlensing and imaging planets, the sky-projected orbital distance is plotted

(19 and 30 AU, respectively) and only six are beyond 2 AU. At very short periods ( $P < 1$  day), there is a population of lava worlds which are as common as hot Jupiter (Sanchis-Ojeda et al. 2014).

Another type of planets that has no equal in our Solar System is the super-Earth group. These are defined as planets ranging from 1 to 2.5 times the radius of the Earth and/or up to 10 Earth masses. Together with sub-Neptune planets, these seem to be the more abundant planetary types in the galaxy, and were unknown to us only a few years ago (Mayor et al. 2011; Dressing and Charbonneau 2013; Howard et al. 2012; Zeng and Sasselov 2014).

## Characterization of Planetary Atmospheres

With the wealth of exoplanets discovered to date, the time of focusing on detecting new planets is passing, except for finding new planets around the brightest stars. Such is the science case for TESS (Ricker 2016) and PLATO (Ragazzoni et al. 2016) space missions and for several ground based planet searches – such as MASCARA (Snellen et al. 2013), TRAPPIST (Gillon et al. 2011) or KELT (Siverd et al. 2009), among others. The goal is the discovery of targets suitable for in-depth study of their atmospheres, ultimately leading, perhaps, to the detection of biosignatures in

Earth-like worlds (see Sanchez-Lavega 2011 for a general textbook on planetary atmospheres).

The atmospheric characterization of planets can be done by:

- (i) The direct detection of their reflected or emitted light; or by
- (ii) Observing the planet during a transit to derive its atmosphere's transmission spectrum.

The latter method is naturally restricted to planets that transit the star, but it is technically less challenging with currently available instrumentation and techniques.

So far transmission spectroscopy studies have provided a wealth of results for hot Jupiter- and Neptune-size planets, allowing the detection of atmospheric Na, K, HI, CII, OI, H<sub>2</sub>O, CH<sub>4</sub>, CO, and CO<sub>2</sub> (Ehrenreich et al. 2006; Borucki et al. 2010; Tinetti et al. 2010; Sing et al. 2011, 2016; Huitson et al. 2013; Murgas et al. 2014), among many others. And this will probably be extended down to the warm super-Earth regime by the upcoming JWST mission (Beichman et al. 2014; Deming et al. 2009). The direct detection of planetary light has been so far only accomplished for widely separated, young massive planets (Chauvin et al. 2004; Marois et al. 2008) or via high-resolution spectroscopy of hot Jupiters around bright stars (Martins et al. 2015).

For the planets of our Solar System, direct detection of planetary reflected and emitted light is trivial and has been conducted for centuries, but the observations of Solar System planets as transiting objects is more complex, requiring the observation of scarce and time-critical direct transits in front of the Sun, the use of other moons or rings as “mirrors,” or the need to combine multiple observations from in situ platforms.

---

## Solar System Planets in Reflected Light

The Solar System planets and satellites are commonly studied by the direct observation of the light reflected by their atmospheres and surfaces. These include telescope observations and data collected by space missions, which have allowed the characterization of the chemical composition of their atmospheres (Irwin 2003; Niemann et al. 2005, 2010); their dynamics, clouds, and albedo variations (Atreya et al. 2006; Wilson and Atreya 2009); and their evolution over time (Pepin 2006; Baines et al. 2013; Mahaffy et al. 2013).

The atmospheres of the terrestrial planets are dominated by N<sub>2</sub>, in the case of Earth and Titan, whereas for Venus and Mars, the principal component is CO<sub>2</sub>. The giant planets have atmospheres dominated by H<sub>2</sub> and He in around the solar proportions, with heavier elements approximately 4 times the solar value for Jupiter, 10 times for Saturn, and 40 times for Uranus and Neptune (Irwin 2003).

The exploration of the Solar System has uncovered spectacular features. Just as an example, the Cassini spacecraft has observed lightning storms (Fischer et al. 2016), atmospheric turbulences, auroras and thunderstorms, volcanic eruptions

(Bagenal et al. 2016), ringlets and braided rings, strong zonal winds, and interlaced ring and moons systems. The imaging or detection of these features in exoplanets is not possible with current facilities. However, lightning-induced radio emission has been observed in Solar System planets and has been proposed as source of radio excess during transit observations of the exoplanet HAT-P-11b (Hodosán et al. 2016), for instance.

Of special interest is the computation of globally integrated phase curves, which might be within the technical reach of JWST (Gardner et al. 2006). Illumination phase functions, magnitudes, and albedos for Solar System planets have been recently taken by Mallama et al. (2017) covering 7 Johnson-Cousins and 5 principal Sloan bands. Photometric phase curves for Mercury, Venus, Mars, Jupiter, and Saturn have been known for a long time (Irvine et al. 1968) and have allowed the characterization of their cloud systems, albedo, and atmospheric components scattering properties. The empirically derived phase curves of terrestrial planets strongly distinguish between airless Mercury, cloud-covered Venus, and the intermediate case of Mars (Mallama 2009). For giant planets, Mayorga et al. (2016) provided analytic fits to Jupiter's phase function in multiple optical bandpasses by Cassini/Imaging Science Subsystem (ISS). They determined its empirical phase curves from 0 to 140°. These measurements are of interest for studying the energy balance of Jupiter and understanding the scattering behavior of the planet as an exoplanet analog.

In the case of Neptune, Kepler Space Telescope yielded a light curve of the planet determining a significant signature from discrete cloud features. The data were contrasted with disk-resolved imaging from the Keck 10-m and the Hubble Space Telescope. The results suggested that clouds control the character of substellar atmospheric variability and that atmospheres dominated by a few large spots may show inherently greater light curve stability than those which exhibit a greater number of smaller features (Simon et al. 2016).

As the field of exoplanet science moves slowly toward the direct imaging of planets in reflected light, observations of Solar System planets under similar viewing geometries and at similar wavelengths will provide an important framework for interpretation.

It is beyond the scope of this paper to review our knowledge on the Solar System bodies, and we refer for details to previous chapters of this Handbook. In the coming section, however, we pay special attention on the Earth as an exoplanet (the only nontrivial observation).

## Reflected Light of Earth and Earthshine

One of the most important consequences of space exploration was the capability to observe our own Earth. Routinely, plankton blooms, city night lights, and crop health indexes are measured from space. However, when observing it as an exoplanet, i.e., from an astronomical distance, all the reflected solar light and radiated emission from its surface and atmosphere is integrated into a single point

(the *pale blue dot* introduced by Sagan), and most of these features disappear in the noise as global averages are taken. Therefore, to interpret the spatially integrated observations of Earth analogs, one needs to be able to compare them with equivalent data with similar resolution of our planet, the only planet that we know to be inhabited. Over the last years, a variety of studies, both observational and theoretical, to determine how the Earth would look like to an extrasolar observer have been carried out.

Satellites in low-Earth orbit view only a small fraction of the Earth's surface at once so that many observations must be combined to obtain global-scale information (Gibson et al. 1990; Stephens et al. 1981), and it is a major technical and logistical challenge to keep calibrated their instrumentation in orbit. But globally integrated observations of Earth from space have been taken in many occasions from different spacecrafts; see, for instance, Table 3.1 in Vázquez et al. (2010) for a summary.

One of the first observations was made by Sagan et al. (1993); the authors analyzed very low-resolution spectrophotometry taken from the Galileo spacecraft (the Jupiter orbiter) flyby of Earth on December 1990. They found evidences of abundant oxygen and methane coexisting in the atmosphere in strong chemical disequilibrium, a necessary, but not sufficient condition to harbor life (Hitchcock and Lovelock 1967). The signal of the chlorophyll, with a sharp absorption edge at around 750 nm, was also found. The coexistence of these features suggested the evidence of life on Earth.

More recently, Cowan et al. (2009) performed principal components analysis in order to determine if it was possible to identify surface features such as oceans and continents from the EPOXI data. They were able to reconstruct a longitudinally averaged map of the Earth's surface. Crow et al. (2011) were able to categorize Earth among the planets of the Solar System by using visible colors. Also using EPOXI data, Kawahara and Fujii (2010, 2011) and Fujii and Kawahara (2012) proposed an inversion technique which allowed them to sketch two-dimensional planetary albedo maps from annual variations of the disk-integrated scattered light.

The observation of the Earth as a distant planet from the ground is also possible despite our geocentric position by observing the Earthshine (Fig. 2), and this has been reported in a number of works (Woolf et al. 2002; Arnold et al. 2002; Montañés-Rodríguez et al. 2005, 2006; Tinetti et al. 2006a; González-Merino et al. 2013, among others). In these studies, the Earth's reflectance is analyzed by observing the Earthshine, the ghostly glow on the nightly side of the Moon visible to a nighttime observer from Earth when the lunar phase is near new moon (Goode et al. 2001b). This glow is sunlight reflected from the Earth and retroreflected from the lunar surface offering an alternative route to study Earth's atmosphere at a global scale, which was already proposed almost 100 years ago (see Goode et al. (2001b) and references therein). This method proved a reliable technique to measure the Earth effective albedo and to determine from there an accurate value for the planetary albedo (Pallé et al. 2004), which is a crucial parameter in a planet's energy balance.

The visible spectrum of the Earthshine has been studied by several authors (Goode et al. 2001a; Woolf et al. 2002; Qiu et al. 2003; Pallé et al. 2003, 2004),



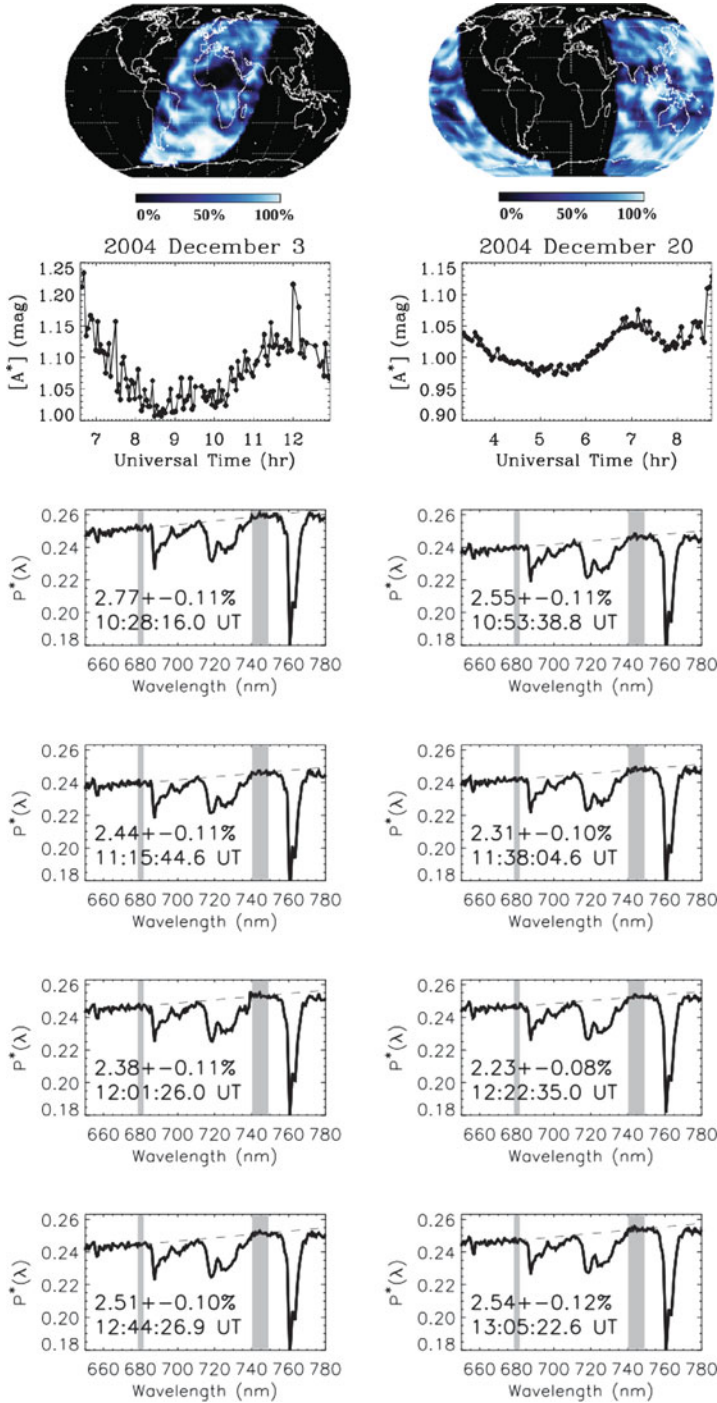


Fig. 2 (continued)



while more recent studies have extended these observations to the near-infrared and to the near-UV. Several authors have also attempted to measure the characteristics of the reflected spectrum and the enhancement of Earth's reflectance at 700 nm due to the presence of vegetation (the possibility of occurrence and detectability was proposed by Wolstencroft and Raven 2002) known as red edge directly (Arnold et al. 2002; Woolf et al. 2002; Seager et al. 2005; Montañés-Rodríguez et al. 2006; Hamdani et al. 2006) and also by using simulations (Tinetti et al. 2006a; Tinetti et al. 2006b; Montañés-Rodríguez et al. 2006). Furthermore, Pallé et al. (2008) determined that the light scattered by the Earth as a function of time contains sufficient information, even with the presence of clouds, to accurately measure Earth's rotation period. More recently, Sterzik et al. (2012) and Miles-Páez et al. (2014) have also studied the use of the linear polarization content of the Earthshine to detect atmospheric species and biosignatures and were able to determine the global fraction of clouds, oceans, and even vegetation.

---

## Transmission Spectroscopy and Solar System

Early Solar System observers already noticed that stars disappear gradually when occulted by a planet and recognized this as a proof of the existence of an atmosphere (Webster 1927). Similarly, the primary and secondary transits of a planet across a star can be used to probe the planetary atmosphere. During a (primary) transit, a small fraction of the stellar flux is blocked by the planet. Part of this fraction passes across the annulus of the planetary atmosphere printing its absorption signatures in the transmitted flux. This is the basis of exoplanet transmission spectroscopy. The secondary transit (or occultation) occurs when the planet passes behind the star, and a measurement of the planet thermal emission and associated features can be achieved, allowing exoplanet emission spectroscopy. Both techniques provide the atmospheric composition. In the first case, the scattering properties of atmospheric components are also obtained, and in the case of the secondary eclipse, the temperature structure can be derived.

The transmission spectrum probes only the outer layers of the planetary atmosphere due to the refracted light. Refraction has an important effect on transmission spectroscopy (García Muñoz et al. 2012), since it removes much of the mid-transit



**Fig. 2** Four upper panels: Earthshine-contributing areas of the Earth for two nights, 2004 December 3 (left), with phase angle 71, and 2004 December 20 (right), with phase angle +60. Apparent terrestrial albedo ( $[A^*]$ ) for these two nights are also respectively shown. Bottom panels: Evolution of the Earthshine spectrum during observations on 2003 November 19. Shaded strips in each panel indicate the two sectors used to determine the red-edge slope. The percentage rise between 680 and 740 nm and the time of observation (UT) are also indicated. The narrow strip in each panel is a continuum region that does not show much variation. Various spectral positions and widths of the narrow band of continuum were tried with similar results for the relative increase of the red-edge bump. The dashed line in each panel connecting the broad and narrow strips indicates the slope from which the change in intensity in the red edge is determined (Adapted from Montanes Rodriguez 2006)

structure in the spectrum. This introduces a maximum tangent pressure level that can be probed during a transit. For Earth around a Sun-like star, for instance, this is 0.3 bar (Misra and Meadows 2014), whereas for an Earth-like planet around an M5V star, almost the whole atmosphere could be probed.

In preparation for the interpretation of transmission spectroscopy data from exoplanets, a number of experimental observations of Solar System bodies have been taken, trying to replicate the observational geometry. Here we review them planet by planet.

## Transit of Mercury

Mercury transits are relatively frequent, typically 13 or 14 per century, the last one occurring on 9 May 2016 (Pasachoff et al. 2016) (Fig. 3). However, Mercury does not provide a very interesting transiting target, due to its really tenuous atmospheres. Nevertheless, the observations of Mercury transits have become a powerful tool for studying the planet's sodium exosphere (Potter et al. 2013), since they allow the detection of excess absorption in the solar sodium lines  $D_1$  and  $D_2$ , as measured during its 2003 transit (Schleicher et al. 2004). This results were later confirmed during the 2006 Mercury transit (Yoshikawa et al. 2008).

## Transit of Venus

Observations of the transits of Venus carry a rich history of astronomical discovery and exciting science, which are amply discussed in Kurtz (2005). In fact, Venus's atmosphere was discovered by observing a transit in front of the Sun (Pasachoff and Sheehan 2012). For the first time after the detection of exoplanets, Venus transited the Sun on 8 June 2004 and on 6 June 2012. These events were the only

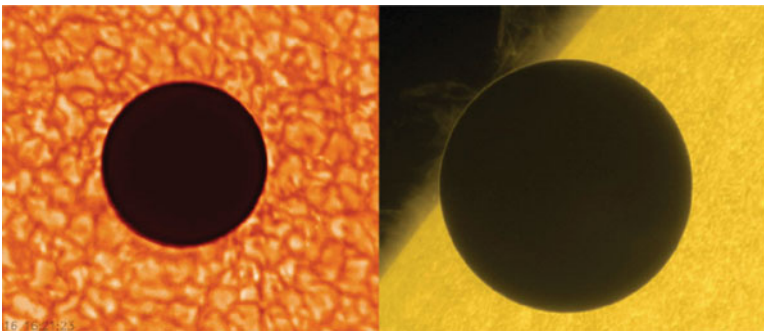


**Fig. 3** Left: Sample image from the Big Bear Solar Observatory's transit of Mercury observations on 2016 using adaptive optics (Image credit: NJIT/BBSO). Right: Sample image of Hinode Mission's observations of the transit of Venus on 2012 (Image credit: JAXA/NASA)

transits directly observable from the Earth during this century, of a planet with an atmosphere in front to the Sun. This offered an opportunity to observe Venus as an exoplanet and try to measure the composition of its atmosphere using the transit method (Ehrenreich et al. 2012).

Naturally, observations were carried out from space and Solar Telescopes all around the world. However, most of the available instruments were typically designed to cover a very narrow spectral range or to obtain photometric images of the events. Simultaneous optical, ultraviolet, and X-ray image observations were carried out by Reale et al. (2015) during the 2012 transit. They analyzed the observations of the Solar Dynamics Observatory/Atmospheric Imaging Assembly (AIA) in the optical (4,500 Å), ultraviolet (1,600 and 1,700 Å), and extreme ultraviolet (171, 193, 211, 304, and 335 Å) channels and of the Hinode/X-Ray Telescope (XRT)16 in the Ti-poly filter that has the maximum sensitivity at 10 Å to determine the planet radius using the radial intensity profiles.

Several attempts were done to obtain an entire UV-VIS-NIR transmission spectrum of Venus from the 2012 transit without conclusive results. The only insight into the Venus atmosphere was detected using the Tenerife Infrared Polarimeter (TIP) at the Vacuum Tower Telescope (VTT) in Tenerife, with which the transit of Venus in June 2004 was observed. The molecular absorption lines of the three most abundant CO<sub>2</sub> isotopologues <sup>12</sup>C<sup>16</sup>O<sub>2</sub>, <sup>13</sup>C<sup>16</sup>O<sub>2</sub>, and <sup>12</sup>C<sup>16</sup>O<sup>18</sup>O and their relative abundances within the atmosphere of Venus were detected (Hedelt et al. 2011). Moreover, the observations resolved Venus' limb, showing Doppler-shifted absorption lines that are probably caused by high-altitude winds.

Stellar activity and convection-related structures in the stellar photosphere cause fluctuations that can affect the transit light curves. Chiavassa et al. (2015) developed surface convection simulations for the Sun to interpret the 2004 transit of Venus, which can help to understand other transits outside our Solar System. They quantified the uncertainty introduced by granulation on the transit light curve as  $9.1 \times 10^5$ .

## Transit of the Earth

The characterization of spectral features in our planet's transmission spectrum can be achieved through (i) the observation from space of Earth's transits in front of the Sun (never obtained so far) or (ii) ground-based observations of the light reflected from the Moon toward the Earth during lunar eclipses. This latter method resembles the observing geometry during a planetary transit.

During a lunar eclipse, the reflected sunlight from the lunar surface within the Earth's umbra will be entirely dominated by the fraction of sunlight that is transmitted through an atmospheric ring located along the Earth's day-night terminator. Except for some early attempts with photographic plates (Slipher 1914; Moore and Brigham 1927), spectroscopic lunar eclipse observations in visible or near-infrared wavelengths had not been undertaken until recently. Observations of the lunar eclipse on 16 August 2008 allowed (Pallé et al. 2009) to characterize

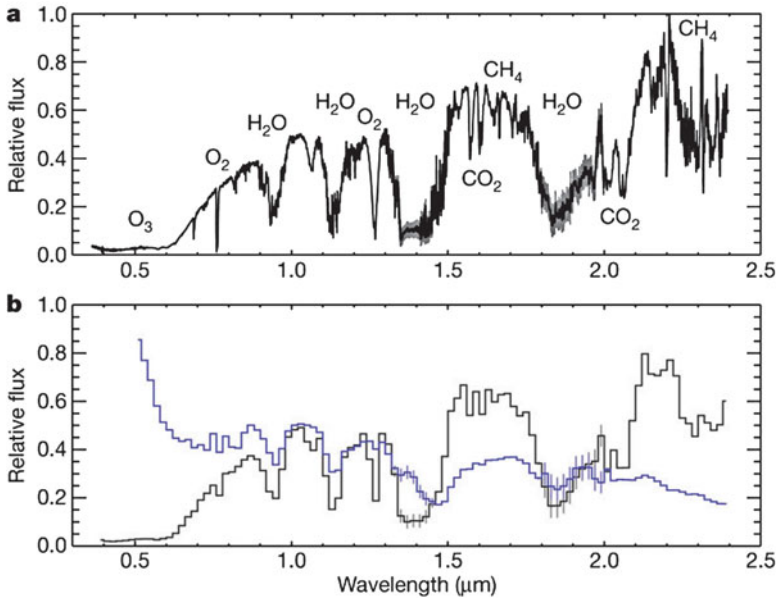


**Fig. 4** The Earth's transmission spectrum is a proxy for Earth observations during a primary transit as seen beyond the Solar System, while the reflection spectrum is a proxy for the observations of Earth as an exoplanet by direct observation after removal of the Sun's spectral features. Top panel: The transmission spectrum, with some of the major atmospheric constituents marked. Bottom panel: A comparison between the Earth's transmission (black) and reflection (blue) spectra. Both spectra have been degraded to a spectral resolution of  $0.02 \mu\text{m}$  and normalized at the same flux value at around  $1.2 \mu\text{m}$  (Adapted from Pallé et al. 2009)

the Earth's spectrum as if it were observed from an astronomical distance during a transit in front of the Sun. Some biologically relevant atmospheric features that are weak in the reflection spectrum (such as ozone, molecular oxygen, water, carbon dioxide, and methane) were found to be much stronger in the transmission spectrum. Moreover, they also found that the spectrum contains the dimer signatures of the major atmospheric constituent, molecular nitrogen ( $N_2$ ), which are missing in the reflection spectrum. This latter feature has been proposed as a proxy to resolve atmospheric pressure on exoplanet atmospheres (Misra et al. 2014).

The Earth's transmission and reflection spectra are plotted in Fig. 4. It is readily seen from the figure that the reflection spectrum shows increased Rayleigh reflectance in the blue. It is also noticeable how most of the molecular spectral bands are weaker, and some nonexistent, in the reflection spectrum.

The measure of the Rossiter-McLaughlin (RM) effect is another technique used to characterize transiting planets. When a body passes in front of a star, the consequent occultation of a small area of the rotating stellar surface produces a distortion of the stellar line profiles, which can be measured as a drift of the radial velocity. The phenomenon was observed in eclipsing binaries by McLaughlin (1924) and Rossiter (1924) and in the Jupiter-like planets (Queloz et al. 2000). But

the amplitude of the RM effect is related to the radius of the planet which, because of differential absorption in the planetary atmosphere, depends on wavelength. Therefore, the wavelength-dependent RM effect can be used to probe the planetary atmosphere (Snellen 2004). In the case of a lunar eclipse, the photon signal-to-noise ratio is so large that this technique can be explored for future applications with extremely large telescopes to exoplanets. Yan et al. (2015b) measure for the first time the RM effect of the Earth transiting the Sun using a lunar eclipse observed with the HARPS spectrograph. The ozone Chappuis band absorption and the Rayleigh scattering features were clearly detectable with this technique.

The last transit of Earth as seen from Mars was in 1984, with no human testimony, but if any of the rough plans for sending humans to Mars becomes a reality, then on November 10, 2084, Martian explorers might directly observe the first transit of an inhabited planet crossing the Sun.

## Transit of Mars

Mars is further from the Sun than the Earth, and thus it is not possible to directly observe Mars as a planet transiting the solar disc. However, a similar technique as for the Earth's could be applied, as it has been done also for Jupiter and Saturn (see next sections).

The small Martian satellites Phobos and Deimos orbit Mars in synchronous rotation with inclinations of only 0.01 deg and 0.92 deg relative to the planet's equatorial plane. Therefore, an observer at near-equatorial latitudes on Mars could occasionally observe the transit of the satellites in front of the solar disk or cross the planet's shadows. This was already done by the Viking spacecraft that observed the shadow of Phobos moving across the landscape in the 1970s and by the Mars Pathfinder that observed Phobos emerge at night from the shadow of Mars in 1997 (Murchie 1999). These data can be used for correcting and refining the orbital ephemerids of the moons. They have also been measured more recently by the two MER Rovers, Spirit and Opportunity, and continue to be taken by Opportunity (which remains active as of August 31, 2017) using the Pancam system (Duxbury et al. 2014; Bell et al. 2005).

The observation of the spectrum of Phobos or Deimos into the Mars shadow has never been observed from Earth. This is a difficult accomplishment, given Mars' orbit relative to Earth, the small size of its moons, and the small signal transmitted by its atmosphere. However, three eclipse ingresses by Phobos into Mars shadow were observed during April–June 2015 by the Mars Science Laboratory's Mastcam, from the Curiosity, by solar occultation photometry (Lemmon 2015). Each eclipse was imaged with both Mastcam cameras, M-100 with an RGB filter (638, 551, and 493 nm) and M-34 with an 867-nm filter. Four events showed significantly higher extinction in the blue, with a monotonic decrease with wavelength, interpreted as a result of 0.3–0.4  $\mu\text{m}$  dust aerosols. Two events (one of each type) showed no significant wavelength variation of extinction, interpreted as a result of large ( $>1 \mu\text{m}$ ) aerosols. One of these, probing local sunrise conditions, may suggest a thin layer of  $\text{CO}_2$  ice clouds.

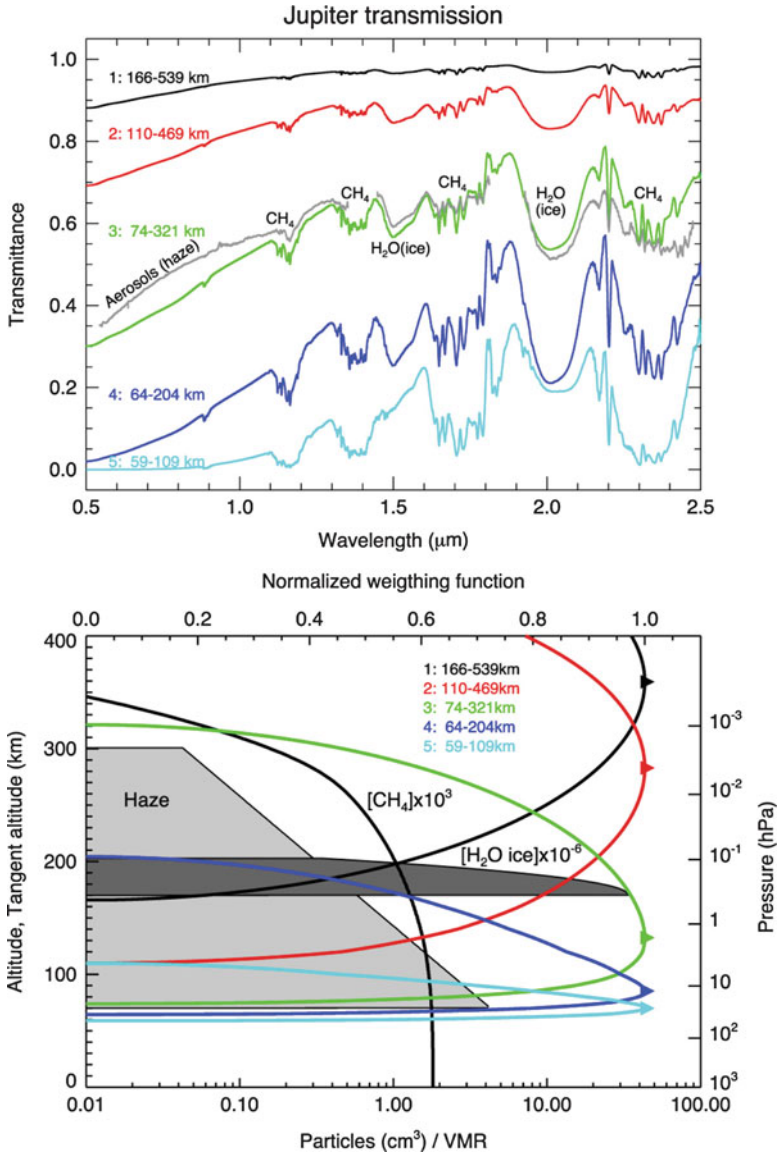


**Fig. 5** Top: Transmission spectra of Jupiter calculated for the early phase of the penumbra and at several stages during the umbra over the 0.5–2.5  $\mu\text{m}$  spectral region (Montañés-Rodríguez et al. 2015). The spectra show the most prominent  $\text{CH}_4$  bands, the extinction of the aerosol particles (haze), and the two distinct absorption peaks of water ice at 1.5 and 2.0  $\mu\text{m}$ . Plotted with a gray line is one of the observed spectra close to the umbra phase. Bottom: An illustration of the distribution of haze,  $\text{CH}_4$ , and  $\text{H}_2\text{O}$  ice in our model, together with geometrical information on the range of tangent altitudes covered in each of our simulations in the top panel, corresponding to the mean times when the (umbra)-penumbral spectra were taken. Altitude is taken as zero at the 1 bar pressure level. In addition, the authors have overplotted the profiles of the concentrations of aerosols and of the water-ice particle cloud used in the computation of the transmission spectra. Note how the sounded region shrinks as the eclipse progresses while moving down to lower tangent heights

## Transit of Jupiter

The transmission spectrum of Jupiter, as if it was a transiting exoplanet, has been recently obtained by observing its satellites while passing through Jupiter's shadow, i.e., during a solar eclipse from the satellite (Montañés-Rodríguez et al. 2015). This methodology was applied to two different eclipses of Ganymede during its crossing of Jupiter's shadow. The observations were done from two different ground locations and instrumentation; in October 2012, an eclipse was observed using LIRIS at the WHT in La Palma Observatory, and in November 2012, another one was observed with XSHOOTER at the VLT in Paranal Observatory. The latter allowed a covering from 300 to 2500 nm in a single exposure through a dichroic splitting of the beam (Fig. 5).

The penumbra transmission spectra of the planet were determined by calculating the ratio between the spectra taken during the penumbra and the spectra taken before the eclipse, i.e., when the satellite is fully illuminated by sunlight. The umbra transmission spectra were determined by calculating the ratio between the spectra taken during umbra and the spectra taken just before eclipse. These ratios cancel the telluric contribution of the local atmosphere, the solar spectrum intrinsic in the observations, and the spectral signatures of the satellite (Montañés-Rodríguez et al. 2006; Pallé et al. 2009; Yan et al. 2015a), leaving only the contribution from Jupiter's atmosphere. The results reveal the imprints of strong extinction due to the presence of clouds (aerosols) and hazes in Jupiter's atmosphere and strong absorption features from CH<sub>4</sub>. More interestingly, the comparison with radiative transfer models (KOPRA; Stiller 2000) reveals a spectral signature, which is attributed to a stratospheric layer of crystalline H<sub>2</sub>O ice. The atomic transitions of Na are also present.

From space, Formisano et al. (2003) analyzed observations made by the Cassini VIMS experiment during the Jupiter flyby of December/January 2000/2001. At the time, Io was within the shadow of Jupiter and was illuminated only by solar light which had transited the atmosphere of Jupiter. This light, therefore, becomes imprinted with the spectral signature of Jupiter's upper atmosphere, which includes strong atmospheric methane absorption bands (Formisano et al. 2003).

## Transit of Saturn

Formisano et al. (2003) foresaw a nearly continuous multi-year period of eclipse events at Saturn, utilizing the large and bright ring system during Cassini's 4-year nominal mission. These data have not been yet presented in the literature, but Dalba et al. (2015) used solar occultations observed by the Visual and Infrared Mapping Spectrometer on board the Cassini Spacecraft to extract the 1–5 μm transmission spectrum of Saturn. Atmospheric absorption signatures from methane, ethane, acetylene, aliphatic hydrocarbons, and possibly carbon monoxide, were detected, with peak-to-peak features of up to 90 parts-per-million despite the presence



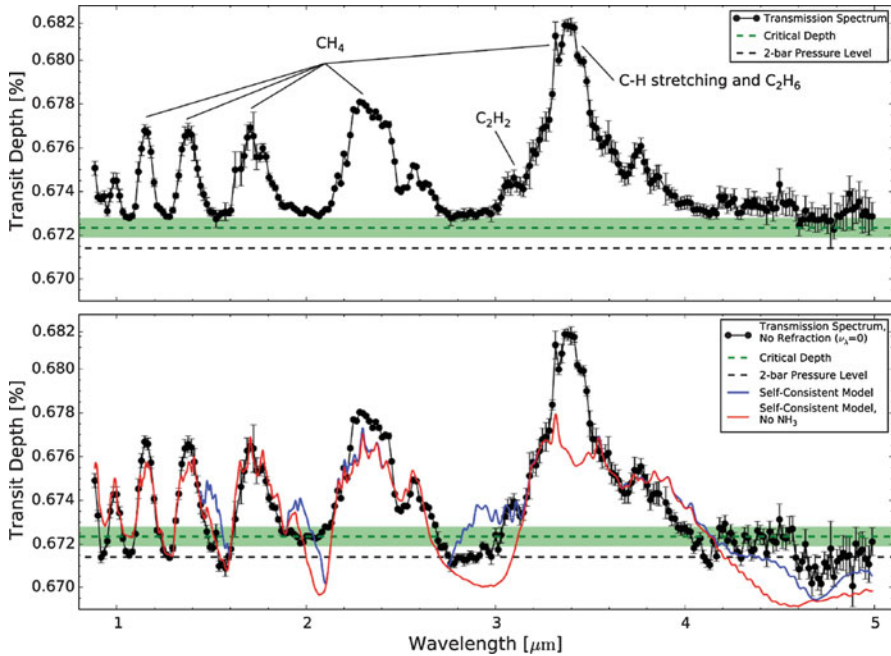


**Fig. 6** Top: Near-infrared, transmission spectrum of Saturn (black data points). The error bars are the 1 uncertainties, which in some cases are smaller than the data point. The dashed green line and shaded green region correspond to the critical altitude and 1 uncertainty range, below which rays cannot probe during mid-transit due to atmospheric refraction. The dashed black line corresponds to the two-bar pressure level in the models and presumably the top of Saturn's global  $\text{NH}_3$  cloud layer. Bottom: Saturn's transmission spectrum generated without the effects of refraction. In this scenario, the base of the spectrum is set by a gray opacity source near the two-bar level and not the critical depth. Two self-consistent atmosphere models (blue and red) are plotted with the transmission spectrum. The blue model allows for  $\text{NH}_3$  in gaseous form, while the red model forces the gaseous  $\text{NH}_3$  content to zero. These models do not include the critical altitude set by refraction or the gray opacity source near two bars (Adapted from Dalba et al. 2015)

of ammonia clouds. Importantly, they also found that atmospheric refraction, as opposed to clouds or haze, determines the minimum altitude that can be probed during mid-transit (Fig. 6).

## Transit of Titan

Although Titan is not a planet, this Saturn's moon is an primary object for astrobiological studies, due to its similarity to the early Earth atmosphere and the presence of liquid bodies in its's surface. Titan's atmosphere has an important haze effect that extends to pressures approaching the  $10^{-6}$  bar level (Brown et al. 2010)

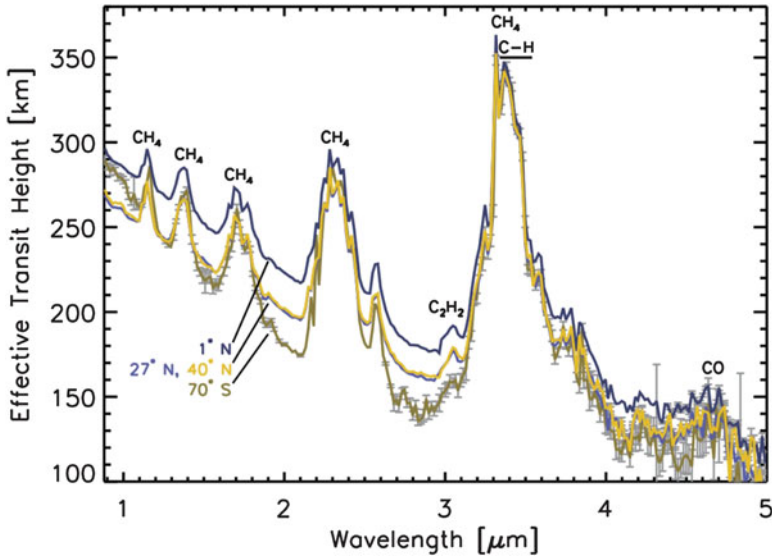


**Fig. 7** Spectra of effective transit height,  $z_{\text{eff},\lambda} = R_{\text{eff},\lambda} R_p$ , for all four Cassini/VIMS occultation datasets. Key absorption features are labeled, and error bars are shown only where the  $1\sigma$  uncertainty is larger than 1%. The best fit haze model for the  $70^\circ$  S dataset is shown (dashed line) (Adapted from Robinson et al. 2014)

and, unlike exoplanets, is extremely well-studied, including in situ observations (Porco et al. 2005).

In Robinson et al. (2014), the authors used solar occultation observations of Titan’s atmosphere from the Visual and Infrared Mapping Spectrometer aboard National Aeronautics and Space Administration’s (NASA) Cassini spacecraft to generate transit spectra. Data span  $0.88\text{--}5\ \mu\text{m}$  at a resolution of  $12\text{--}18\ \text{nm}$  (Fig. 7). The retrieved spectra showed strong methane absorption features and weaker features corresponding to other gases. Most importantly, the data demonstrated that high-altitude hazes can severely limit the atmospheric depths probed by transit spectra, introducing slopes in the spectra and bounding observations to pressures smaller than  $0.1\text{--}10\ \text{m bar}$ , depending on wavelength.

High-altitude clouds and hazes are integral to understanding exoplanet observations and are proposed to explain observed featureless transit spectra. The observations of Titan highlight just how important this phenomena.

## Transits of Uranus and Neptune

Unfortunately, the outer two ice giant planets have no moons suitable for recording transmission spectroscopy. Only the shadow of Ariel in front of Uranus has been recorded, during a primary transit of this moon ([hubblesite.org/newsrelease/news/](http://hubblesite.org/newsrelease/news/)

2006-42). Thus, Uranus or Neptune *as planets* remains to be explored using the technique described for inner planets.

## Concluding Remarks

Over the past decades, a large diversity in planetary systems, accompanied by a large diversity of planetary natures, have been uncovered. Nevertheless, despite probable surprises, our knowledge of the Solar System planets will be our first reference frame in the interpretation of the physical properties of extrasolar planet atmospheres. Thus, the Solar System offers a unique playground to determine the best observables for such planet characterization. All Solar System planets can be observed in reflected/emitted light with much more detail than we hope to archive in exoplanetary atmospheres for many decades. On the other hand, transmission spectroscopy is currently the less technically challenging technique to explore exoplanet atmospheres and has led to the first successful detections of molecular and atomic species. However, globally averaged transmission spectroscopy of Solar System planets has not been historically available.

In the past few years, several observations have been performed aimed at retrieving the transmission spectrum of some of the Solar Systems planets. These observations include the transmission spectrum of Venus while transiting the Sun, the Earth (via a lunar eclipse), Jupiter (via a Ganymedes eclipse and in situ measurements), and Saturn. Together they have revealed a wealth of new information, such as the detectability of dimer bands (usable as tracers of atmospheric pressure) in Earth-like planets or the signatures of aerosols, hazes, and metallic layers in giant planets. In the near future, detailed observations expanding the wavelength coverage, the time domain variability, and the inclusion of the remaining Solar System planets will surely provide a more complete picture with which to interpret new exoplanet discoveries.

**Acknowledgements** This work is partly financed by the Spanish Ministry of Economics and Competitiveness through projects ESP2014-57495-C2-1-R and ESP2016-80435-C2-2-R.

---

## References

- Alessi M, Pudritz RE, Cridland AJ (2017) On the formation and chemical composition of super Earths. *MNRAS* 464:428–452. <https://doi.org/10.1093/mnras/stw2360>, 1606.09174
- Armitage PJ (2007) Massive planet migration: theoretical predictions and comparison with observations. *ApJ* 665:1381–1390. <https://doi.org/10.1086/519921>, 0705.3039
- Armitage PJ (2010) *Astrophysics of planet formation*. Cambridge University Press, Cambridge
- Arnold L, Gillet S, Lardièrre O, Riaud P, Schneider J (2002) A test for the search for life on extrasolar planets. Looking for the terrestrial vegetation signature in the Earthshine spectrum. *A&A* 392:231–237. <https://doi.org/10.1051/0004-6361:20020933>, astro-ph/0206314
- Atreya SK, Adams EY, Niemann HB et al (2006) Titan's methane cycle. *Planet Space Sci* 54: 1177–1187. <https://doi.org/10.1016/j.pss.2006.05.028>

- Bagenal F, Nerney E, Steffl AJ (2016) Io plasma torus ion composition: Voyager, Galileo, Cassini. In: AAS/Division for planetary sciences meeting abstracts, vol 48, p 402.04
- Baines KH, Atreya SK, Bullock MA et al (2013) The atmospheres of the terrestrial planets: clues to the origins and early evolution of Venus, Earth, and Mars, pp 137–160. [https://doi.org/10.2458/azu\\_uapress\\_9780816530595-ch006](https://doi.org/10.2458/azu_uapress_9780816530595-ch006)
- Batalha NM (2014) Exploring exoplanet populations with NASA's Kepler mission. *Proc Natl Acad Sci* 111:12647–12654. <https://doi.org/10.1073/pnas.1304196111>, 1409.1904
- Batygin K, Bodenheimer PH, Laughlin GP (2016) In situ formation and dynamical evolution of hot Jupiter systems. *ApJ* 829:114. <https://doi.org/10.3847/0004-637X/829/2/114>, 1511.09157
- Beichman C, Benneke B, Knutson H et al (2014) Observations of transiting exoplanets with the James webb space telescope (JWST). *PASP* 126:1134. <https://doi.org/10.1086/679566>
- Bell JF, Lemmon MT, Duxbury TC et al (2005) Solar eclipses of Phobos and Deimos observed from the surface of Mars. *Nature* 436:55–57. <https://doi.org/10.1038/nature03437>
- Boley AC, Granados Contreras AP, Gladman B (2016) The in situ formation of giant planets at short orbital periods. *ApJ* 817:L17. <https://doi.org/10.3847/2041-8205/817/2/L17>, 1510.04276
- Bonfils X, Delfosse X, Udry S et al (2013) The HARPS search for southern extra-solar planets. XXXI. The M-dwarf sample. *A&A* 549:A109. <https://doi.org/10.1051/0004-6361/201014704>, 1111.5019
- Borucki WJ, Koch D, Basri G et al (2010) Kepler planet-detection mission: introduction and first results. *Science* 327:977. <https://doi.org/10.1126/science.1185402>
- Brown RH, Lebreton JP, Waite JH (2010) Titan from Cassini-Huygens. <https://doi.org/10.1007/978-1-4020-9215-2>
- Burke CJ (2015) Terrestrial planet occurrence rates for the Kepler GK dwarf sample. In: AAS/Division for extreme solar systems abstracts, vol 3, p 501.01
- Chambers JE (2016) Pebble accretion and the diversity of planetary systems. *ApJ* 825:63. <https://doi.org/10.3847/0004-637X/825/1/63>, 1604.06362
- Chauvin G, Lagrange AM, Dumas C et al (2004) A giant planet candidate near a young brown dwarf. Direct VLT/NACO observations using IR wavefront sensing. *A&A* 425:L29–L32. <https://doi.org/10.1051/0004-6361:200400056>, astro-ph/0409323
- Chiavassa A, Pere C, Faurobert M et al (2015) New view on exoplanet transits. Transit of Venus described using three-dimensional solar atmosphere STAGGER-grid simulations. *A&A* 576:A13. <https://doi.org/10.1051/0004-6361/201425256>, 1501.06207
- Cowan NB, Agol E, Meadows VS et al (2009) Alien maps of an ocean-bearing world. *ApJ* 700:915–923. <https://doi.org/10.1088/0004-637X/700/2/915>, 0905.3742
- Crow CA, McFadden LA, Robinson T et al (2011) Views from EPOXI: colors in our solar system as an analog for extrasolar planets. *ApJ* 729:130. <https://doi.org/10.1088/0004-637X/729/2/130>
- Dalba PA, Muirhead PS, Fortney JJ et al (2015) The transit transmission spectrum of a cold gas giant planet. *Astrophys J* 814(2):154. <http://stacks.iop.org/0004-637X/814/i=2/a=154>
- Deming D, Seager S (2009) Light and shadow from distant worlds. *Nature* 462:301–306. <https://doi.org/10.1038/nature08556>
- Deming D, Seager S, Winn J et al (2009) Discovery and characterization of transiting super Earths using an all-sky transit survey and follow-up by the James webb space telescope. *PASP* 121:952. <https://doi.org/10.1086/605913>, 0903.4880
- Dressing CD, Charbonneau D (2013) The occurrence rate of small planets around small stars. *ApJ* 767:95. <https://doi.org/10.1088/0004-637X/767/1/95>, 1302.1647
- Duxbury TC, Zakharov AV, Hoffmann H, Guinness EA (2014) Spacecraft exploration of Phobos and Deimos. *Planet Space Sci* 102:9–17. <https://doi.org/10.1016/j.pss.2013.12.008>
- Ehrenreich D, Tinetti G, Lecavelier Des Etangs A, Vidal-Madjar A, Selsis F (2006) The transmission spectrum of Earth-size transiting planets. *A&A* 448:379–393. <https://doi.org/10.1051/0004-6361:20053861>, astro-ph/0510215
- Ehrenreich D, Vidal-Madjar A, Widemann T et al (2012) Transmission spectrum of Venus as a transiting exoplanet. *A&A* 537:L2. <https://doi.org/10.1051/0004-6361/201118400>, 1112.0572

- Fernandez JA, Ip WH (1984) Some dynamical aspects of the accretion of Uranus and Neptune – the exchange of orbital angular momentum with planetesimals. *Icarus* 58:109–120. [https://doi.org/10.1016/0019-1035\(84\)90101-5](https://doi.org/10.1016/0019-1035(84)90101-5)
- Fischer G, Paganan J, Dyudina U, Delcroix M (2016) Dynamics of Saturnian thunderstorms. In: EGU general assembly conference abstracts, vol 18, p 6505
- Formisano V, D’Aversa E, Bellucci G et al (2003) Cassini-VIMS at Jupiter: solar occultation measurements using Io. *Icarus* 166:75–84. [https://doi.org/10.1016/S0019-1035\(03\)00178-7](https://doi.org/10.1016/S0019-1035(03)00178-7)
- Fujii Y, Kawahara H (2012) Mapping Earth analogs from photometric variability: spin-orbit tomography for planets in inclined orbits. *ApJ* 755:101. <https://doi.org/10.1088/0004-637X/755/2/101>, 1204.3504
- García Muñoz A, Zapatero Osorio MR, Barrena R et al (2012) Glancing views of the Earth: from a Lunar eclipse to an exoplanetary transit. *ApJ* 755:103. <https://doi.org/10.1088/0004-637X/755/2/103>, 1206.4344
- Gardner JP, Mather JC, Clampin M et al (2006) The James webb space telescope. *Space Sci Rev* 123:485–606. <https://doi.org/10.1007/s11214-006-8315-7>, astro-ph/0606175
- Gibson GG, Denn FM, Young DW et al (1990) Characteristics of the Earth’s radiation budget derived from the first year of data from the Earth radiation budget experiment. In: Barkstrom BR (ed) Long-term monitoring of the Earth’s radiation budget, Proceedings of SPIE, vol 1299, pp 253–263. <https://doi.org/10.1117/12.21383>
- Gillon M, Jehin E, Magain P et al (2011) TRAPPIST: a robotic telescope dedicated to the study of planetary systems. In: European physical journal web of conferences, vol 11, p 06002. <https://doi.org/10.1051/epjconf/20101106002>, 1101.5807
- Gomes R, Levison HF, Tsiganis K, Morbidelli A (2005) Origin of the cataclysmic late heavy bombardment period of the terrestrial planets. *Nature* 435:466–469. <https://doi.org/10.1038/nature03676>
- González-Merino B, Pallé E, Motalebi F, Montañés-Rodríguez P, Kissler-Patig M (2013) Earthshine observations at high spectral resolution: exploring and detecting metal lines in the Earth’s upper atmosphere. *MNRAS* 435:2574–2580. <https://doi.org/10.1093/mnras/stt1463>, 1309.0354
- Goode B, Cary JR, Doxas I, Horton W (2001a) Differentiating between colored random noise and deterministic chaos with the root mean squared deviation. *J Geophys Res* 106:21277–21288. <https://doi.org/10.1029/2000JA000167>
- Goode PR, Qiu J, Yurchyshyn V et al (2001b) Earthshine observations of the Earth’s reflectance. *Geophys Res Lett* 28:1671–1674. <https://doi.org/10.1029/2000GL012580>
- Hamdani S, Arnold L, Foellmi C et al (2006) Biomarkers in disk-averaged near-UV to near-IR Earth spectra using Earthshine observations. *A&A* 460:617–624. <https://doi.org/10.1051/0004-6361:20065032>, astro-ph/0609195
- Hedelt P, Alonso R, Brown T et al (2011) Venus transit 2004: illustrating the capability of exoplanet transmission spectroscopy. *A&A* 533:A136. <https://doi.org/10.1051/0004-6361/201016237>, 1107.3700
- Hitchcock DR, Lovelock JE (1967) Life detection by atmospheric analysis. *Icarus* 7:149–159. [https://doi.org/10.1016/0019-1035\(67\)90059-0](https://doi.org/10.1016/0019-1035(67)90059-0)
- Hodosán G, Rimmer PB, Helling C (2016) Is lightning a possible source of the radio emission on HAT-P-11b? *MNRAS* 461:1222–1226. <https://doi.org/10.1093/mnras/stw977>, 1604.07406
- Howard AW, Marcy GW, Bryson ST et al (2012) Planet occurrence within 0.25 AU of solar-type stars from kepler. *ApJS* 201:15. <https://doi.org/10.1088/0067-0049/201/2/15>, 1103.2541
- Huitson CM, Sing DK, Pont F et al (2013) An HST optical-to-near-IR transmission spectrum of the hot Jupiter WASP-19b: detection of atmospheric water and likely absence of TiO. *MNRAS* 434:3252–3274. <https://doi.org/10.1093/mnras/stt1243>, 1307.2083
- Ip WH, Fernandez JA (1988) Exchange of condensed matter among the outer and terrestrial protoplanets and the effect on surface impact and atmospheric accretion. *Icarus* 74:47–61. [https://doi.org/10.1016/0019-1035\(88\)90030-9](https://doi.org/10.1016/0019-1035(88)90030-9)
- Irvine WM, Simon T, Menzel DH, Pikoos C, Young AT (1968) Multicolor photoelectric photometry of the brighter planets. III. Observations from Boyden observatory. *AJ* 73:807. <https://doi.org/10.1086/110702>

- Irwin PGJ (2003) Giant planets of our solar system: atmospheres compositions, and structure. Springer, Berlin/Heidelberg. <https://doi.org/10.1007/978-3-540-85158-5>
- Kawahara H, Fujii Y (2010) Global mapping of Earth-like exoplanets from scattered light curves. *ApJ* 720:1333–1350. <https://doi.org/10.1088/0004-637X/720/2/1333>, 1004.5152
- Kawahara H, Fujii Y (2011) Mapping clouds and terrain of Earth-like planets from photometric variability: demonstration with planets in face-on orbits. *ApJ* 739:L62. <https://doi.org/10.1088/2041-8205/739/2/L62>, 1106.0136
- Kley W, Nelson RP (2012) Planet-disk interaction and orbital evolution. *ARA&A* 50:211–249. <https://doi.org/10.1146/annurev-astro-081811-125523>, 1203.1184
- Kurtz DW (ed) (2005) *Transits of Venus: new views of the solar system and galaxy*. Cambridge University Press, Cambridge
- Laughlin G, Deming D, Langton J et al (2009) Rapid heating of the atmosphere of an extrasolar planet. *Nature* 457:562–564. <https://doi.org/10.1038/nature07649>
- Lee EJ, Chiang E, Ormel CW (2014) Make super-earths, not Jupiters: accreting nebular gas onto solid cores at 0.1 AU and beyond. *ApJ* 797:95. <https://doi.org/10.1088/0004-637X/797/2/95>, 1409.3578
- Lemmon MT (2015) Martian upper atmospheric aerosol properties from phobos eclipse observation. In: AAS/Division for planetary sciences meeting abstracts, vol 47, p 401.09
- Lin DNC, Bodenheimer P, Richardson DC (1996) Orbital migration of the planetary companion of 51 Pegasi to its present location. *Nature* 380:606–607. <https://doi.org/10.1038/380606a0>
- Mahaffy PR, Webster CR, Atreya SK et al (2013) Abundance and isotopic composition of gases in the martian atmosphere from the curiosity rover. *Science* 341:263–266. <https://doi.org/10.1126/science.1237966>
- Malhotra R (1995) The origin of Pluto's orbit: implications for the solar system beyond Neptune. *AJ* 110:420. <https://doi.org/10.1086/117532>, astro-ph/9504036
- Mallama A (2009) Characterization of terrestrial exoplanets based on the phase curves and albedos of Mercury, Venus and Mars. *Icarus* 204:11–14. <https://doi.org/10.1016/j.icarus.2009.07.010>
- Mallama A, Krobusek B, Pavlov H (2017) Comprehensive wide-band magnitudes and albedos for the planets, with applications to exo-planets and planet nine. *Icarus* 282:19–33. <https://doi.org/10.1016/j.icarus.2016.09.023>, 1609.05048
- Marois C, Macintosh B, Barman T et al (2008) Direct imaging of multiple planets orbiting the star HR 8799. *Science* 322:1348. <https://doi.org/10.1126/science.1166585>, 0811.2606
- Martins JHC, Santos NC, Figueira P et al (2015) Evidence for a spectroscopic direct detection of reflected light from 51 Pegasi b. *A&A* 576:A134. <https://doi.org/10.1051/0004-6361/201425298>, 1504.05962
- Mayor M, Queloz D (1995) A Jupiter-mass companion to a solar-type star. *Nature* 378:355–359. <https://doi.org/10.1038/378355a0>
- Mayor M, Marmier M, Lovis C et al (2011) The HARPS search for southern extra-solar planets XXXIV. Occurrence, mass distribution and orbital properties of super-Earths and Neptune-mass planets. *ArXiv e-prints* 1109.2497
- Mayorga LC, Jackiewicz J, Rages K et al (2016) Jupiter's phase variations from Cassini: a testbed for future direct-imaging missions. *AJ* 152:209. <https://doi.org/10.3847/0004-6256/152/6/209>, 1610.07679
- McLaughlin DB (1924) *ApJ* 60:22
- Miles-Páez PA, Pallé E, Zapatero Osorio MR (2014) Simultaneous optical and near-infrared linear spectropolarimetry of the earthshine. *A&A* 562:L5. <https://doi.org/10.1051/0004-6361/201323009>, 1401.6029
- Misra AK, Meadows VS (2014) Discriminating between cloudy, hazy, and clear sky exoplanets using refraction. *ApJ* 795:L14. <https://doi.org/10.1088/2041-8205/795/1/L14>, 1409.7072
- Misra A, Meadows V, Claire M, Crisp D (2014) Using dimers to measure biosignatures and atmospheric pressure for terrestrial exoplanets. *Astrobiology* 14:67–86. <https://doi.org/10.1089/ast.2013.0990>, 1312.2025
- Montanes Rodriguez P (2006) Earth observed as a distant planet. In: *European planetary science congress 2006*, p 573



- Montañés-Rodríguez P, Pallé E, Goode PR, Hickey J, Koonin SE (2005) Globally integrated measurements of the Earth's visible spectral albedo. *ApJ* 629:1175–1182. <https://doi.org/10.1086/431420>, astro-ph/0505084
- Montañés-Rodríguez P, Pallé E, Goode PR, Martín-Torres FJ (2006) Vegetation signature in the observed globally integrated spectrum of Earth considering simultaneous cloud data: applications for extrasolar planets. *ApJ* 651:544–552. <https://doi.org/10.1086/507694>, astro-ph/0604420
- Montañés-Rodríguez P, González-Merino B, Pallé E, López-Puertas M, García-Melendo E (2015) Jupiter as an exoplanet: UV to NIR transmission spectrum reveals hazes, a Na layer, and possibly stratospheric H<sub>2</sub>O-ice clouds. *ApJ* 801:L8. <https://doi.org/10.1088/2041-8205/801/1/L8>
- Moore JH, Brigham LA (1927) The spectrum of the eclipsed moon. *PASP* 39:223. <https://doi.org/10.1086/123720>
- Morbidelli A, Levison HF, Tsiganis K, Gomes R (2005) Chaotic capture of Jupiter's trojan asteroids in the early solar system. *Nature* 435:462–465. <https://doi.org/10.1038/nature03540>
- Morbidelli A, Lunine JI, O'Brien DP, Raymond SN, Walsh KJ (2012) Building terrestrial planets. *Annu Rev Earth Planet Sci* 40:251–275. <https://doi.org/10.1146/annurev-earth-042711-105319>, 1208.4694
- Murchie S (1999) Mars pathfinder spectral measurements of Phobos and Deimos: comparison with previous data. *J Geophys Res* 104:9069–9080. <https://doi.org/10.1029/98JE02248>
- Murgas F, Pallé E, Zapatero Osorio MR et al (2014) The GTC exoplanet transit spectroscopy survey . I. OSIRIS transmission spectroscopy of the short period planet WASP-43b. *A&A* 563:A41. <https://doi.org/10.1051/0004-6361/201322374>, 1401.3692
- Niemann HB, Atreya SK, Bauer SJ et al (2005) The abundances of constituents of Titan's atmosphere from the GCMS instrument on the Huygens probe. *Nature* 438:779–784. <https://doi.org/10.1038/nature04122>
- Niemann HB, Atreya SK, Demick JE et al (2010) Composition of Titan's lower atmosphere and simple surface volatiles as measured by the Cassini-Huygens probe gas chromatograph mass spectrometer experiment. *J Geophys Res (Planets)* 115:E12006. <https://doi.org/10.1029/2010JE003659>
- Pallé E, Goode PR, Yurchyshyn V et al (2003) Earthshine and the Earth's albedo: 2. Observations and simulations over 3 years. *J Geophys Res (Atmos)* 108:4710. <https://doi.org/10.1029/2003JD003611>
- Pallé E, Goode PR, Montañés-Rodríguez P, Koonin SE (2004) Changes in Earth's reflectance over the past two decades. *Science* 304:1299–1301. <https://doi.org/10.1126/science.1094070>
- Pallé E, Ford EB, Seager S, Montañés-Rodríguez P, Vazquez M (2008) Identifying the rotation rate and the presence of dynamic weather on extrasolar Earth-like planets from photometric observations. *ApJ* 676:1319–1329. <https://doi.org/10.1086/528677>, 0802.1836
- Pallé E, Zapatero Osorio MR, Barrena R, Montañés-Rodríguez P, Martín EL (2009) Earth's transmission spectrum from lunar eclipse observations. *Nature* 459:814–816. <https://doi.org/10.1038/nature08050>, 0906.2958
- Pasachoff JM, Sheehan W (2012) Lomonosov, the discovery of Venus's atmosphere, and the eighteenth-century transits of Venus. *J Astron Hist Herit* 15:3–14
- Pasachoff JM, Schneider G, Gary D et al (2016) The 2016 transit of Mercury observed from major solar telescopes and satellites. In: AAS/Division for planetary sciences meeting abstracts, vol 48, p 117.05
- Pepin RO (2006) Atmospheres on the terrestrial planets: clues to origin and evolution. *Earth Planet Sci Lett* 252:1–14. <https://doi.org/10.1016/j.epsl.2006.09.014>
- Porco CC, Baker E, Barbara J et al (2005) Imaging of titan from the cassini spacecraft. *Nature* 434:159–168. <https://doi.org/10.1038/nature03436>
- Potter AE, Killen RM, Reardon KP, Bida TA (2013) Observation of neutral sodium above Mercury during the transit of November 8, 2006. *Icarus* 226:172–185. <https://doi.org/10.1016/j.icarus.2013.05.029>



- Qiu J, Goode PR, Pallé E et al (2003) Earthshine and the Earth's albedo: 1. Earthshine observations and measurements of the lunar phase function for accurate measurements of the Earth's bond albedo. *J Geophys Res (Atmos)* 108:4709. <https://doi.org/10.1029/2003JD003610>
- Queoz D, Eggenberger A, Mayor M et al (2000) *A&A* 359:L13
- Ragazzoni R, Magrin D, Rauk H et al (2016) PLATO: a multiple telescope spacecraft for exoplanets hunting. In: *Space telescopes and instrumentation 2016: optical, infrared, and millimeter wave*. Proceedings of SPIE, vol 9904, p 990428. <https://doi.org/10.1117/12.2236094>
- Reale F, Gambino AF, Micela G et al (2015) Using the transit of Venus to probe the upper planetary atmosphere. *Nat Commun* 6:7563. <https://doi.org/10.1038/ncomms8563>, 1507.00195
- Ricker GR (2016) The transiting exoplanet survey satellite (TESS): discovering exoplanets in the solar neighborhood. AGU fall meeting abstracts
- Robinson TD, Maltagliati L, Marley MS, Fortney JJ (2014) Titan solar occultation observations reveal transit spectra of a hazy world. *Proc Nat Acad Sci* 111:9042–9047. <https://doi.org/10.1073/pnas.1403473111>, 1406.3314
- Rossiter RA (1924) *ApJ* 60:15
- Sagan C, Thompson WR, Carlson R, Gurnett D, Hord C (1993) A search for life on Earth from the Galileo spacecraft. *Nature* 365:715–721. <https://doi.org/10.1038/365715a0>
- Sanchez-Lavega A (2011) *An introduction to planetary atmospheres*. Taylor & Francis Group, LLC. [http://www.ajax.ehu.es/planetary\\_atmospheres://www.ajax.ehu.es/planetary\\_atmospheres/](http://www.ajax.ehu.es/planetary_atmospheres://www.ajax.ehu.es/planetary_atmospheres/)
- Sanchis-Ojeda R, Rappaport S, Winn JN et al (2014) A study of the shortest-period planets found with kepler. *ApJ* 787:47. <https://doi.org/10.1088/0004-637X/787/1/47>, 1403.2379
- Schleicher H, Wiedemann G, Wöhl H, Berkefeld T, Soltau D (2004) Detection of neutral sodium above Mercury during the transit on 2003 May 7. *A&A* 425:1119–1124. <https://doi.org/10.1051/0004-6361:20040477>
- Seager S, Turner EL, Schafer J, Ford EB (2005) Vegetation's red edge: a possible spectroscopic biosignature of extraterrestrial plants. *Astrobiology* 5:372–390. <https://doi.org/10.1089/ast.2005.5.372>, astro-ph/0503302
- Simon AA, Rowe JF, Gaulme P et al (2016) Neptune's dynamic atmosphere from kepler K2 observations: implications for brown dwarf light curve analyses. *ApJ* 817:162. <https://doi.org/10.3847/0004-637X/817/2/162>, 1512.07090
- Sing DK, Pont F, Aigrain S et al (2011) Hubble space telescope transmission spectroscopy of the exoplanet HD 189733b: high-altitude atmospheric haze in the optical and near-ultraviolet with STIS. *MNRAS* 416:1443–1455. <https://doi.org/10.1111/j.1365-2966.2011.19142.x>, 1103.0026
- Sing DK, Fortney JJ, Nikolov N et al (2016) A continuum from clear to cloudy hot-Jupiter exoplanets without primordial water depletion. *Nature* 529:59–62. <https://doi.org/10.1038/nature16068>, 1512.04341
- Sivervd RJ, Pepper J, Stanek K et al (2009) KELT: a wide-field survey of bright stars for transiting planets. In: Pont F, Sasselov D, Holman MJ (eds) *Transiting planets*. IAU symposium, vol 253, pp 350–353. <https://doi.org/10.1017/S1743921308026628>
- Slipher VM (1914) On the spectrum of the eclipsed moon. *Astron Nachr* 199:103
- Snellen IAG (2004) A new method for probing the atmospheres of transiting exoplanets. *MNRAS* 353:L1–L6. <https://doi.org/10.1111/j.1365-2966.2004.08169.x>, astro-ph/0403101
- Snellen I, Stuik R, Otten G et al (2013) MASCARA: the multi-site all-sky CAmERA. In: *European physical journal web of conferences*, vol 47, p 03008. <https://doi.org/10.1051/epjconf/20134703008>
- Stephens GL, Campbell GG, Vonder Haar TH (1981) Earth radiation budgets. *J Geophys Res* 86:9739–9760. <https://doi.org/10.1029/JC086iC10p09739>
- Terzik MF, Bagnulo S, Pallé E (2012) Biosignatures as revealed by spectropolarimetry of Earthshine. *Nature* 483:64–66. <https://doi.org/10.1038/nature10778>
- Stiller GP (ed) (2000) *The Karlsruhe optimized and precise radiative transfer algorithm (KOPRA)*, Wissenschaftliche Berichte, vol FZKA 6487. Forschungszentrum Karlsruhe

- Tinetti G, Meadows VS, Crisp D et al (2006a) Detectability of planetary characteristics in disk-averaged spectra. I: the Earth model. *Astrobiology* 6:34–47. <https://doi.org/10.1089/ast.2006.6.34>
- Tinetti G, Rashby S, Yung YL (2006b) Detectability of red-edge-shifted vegetation on terrestrial planets orbiting m stars. *Astrophys J Lett* 644(2):L129. <http://stacks.iop.org/1538-4357/644/i=2/a=L129>
- Tinetti G, Deroo P, Swain MR et al (2010) Probing the terminator region atmosphere of the hot-Jupiter XO-1b with transmission spectroscopy. *ApJ* 712:L139–L142. <https://doi.org/10.1088/2041-8205/712/2/L139>, 1002.2434
- Tsiganis K, Gomes R, Morbidelli A, Levison HF (2005) Origin of the orbital architecture of the giant planets of the solar system. *Nature* 435:459–461. <https://doi.org/10.1038/nature03539>
- Tuomi M, Anglada-Escudé G (2013) Up to four planets around the M dwarf GJ 163. Sensitivity of Bayesian planet detection criteria to prior choice. *A&A* 556:A111. <https://doi.org/10.1051/0004-6361/201321174>, 1306.1717
- Tuomi M, Jones HRA, Barnes JR, Anglada-Escudé G, Jenkins JS (2014) Bayesian search for low-mass planets around nearby M dwarfs – estimates for occurrence rate based on global detectability statistics. *MNRAS* 441:1545–1569. <https://doi.org/10.1093/mnras/stu358>, 1403.0430
- Vázquez M, Pallé E, Rodríguez PM (2010) *The Earth as a distant planet*. Springer, New York. <https://doi.org/10.1007/978-1-4419-1684-6>
- Walsh KJ, Morbidelli A, Raymond SN, O’Brien DP, Mandell AM (2011) Depletion and excitation of the asteroid belt by migrating planets. In: *Workshop on formation of the first solids in the solar system*, LPI contributions, vol 1639, p 9151
- Walsh KJ, Morbidelli A, Raymond SN, O’Brien DP, Mandell AM (2012) Populating the asteroid belt from two parent source regions due to the migration of giant planets: the grand tack. *Meteorit Planet Sci* 47:1941–1947. <https://doi.org/10.1111/j.1945-5100.2012.01418.x>
- Webster DL (1927) Meteorological, geological, and biological conditions on Venus. *Nature* 120:879–880. <https://doi.org/10.1038/120879a0>
- Wilson EH, Atreya SK (2009) Titan’s carbon budget and the case of the missing ethane. *J Phys Chem A* 113:11221–11226. <https://doi.org/10.1021/jp905535a>
- Winn JN, Fabrycky DC (2015) The occurrence and architecture of exoplanetary systems. *ARA&A* 53:409–447. <https://doi.org/10.1146/annurev-astro-082214-122246>, 1410.4199
- Wolstencroft RD, Raven JA (2002) Photosynthesis: likelihood of occurrence and possibility of detection on Earth-like planets. *Icarus* 157:535–548. <https://doi.org/10.1006/icar.2002.6854>
- Woolf NJ, Smith PS, Traub WA, Jucks KW (2002) The spectrum of earthshine: a pale blue dot observed from the ground. *ApJ* 574:430–433. <https://doi.org/10.1086/340929>, astro-ph/0203465
- Wright JT (2010) Exoplanet orbit database. [www.exoplanets.org](http://www.exoplanets.org)
- Wyatt MC (2008) Evolution of debris disks. *ARA&A* 46:339–383. <https://doi.org/10.1146/annurev.astro.45.051806.110525>
- Yan F, Fosbury R, Petr-Gotzens M, Pallé E, Zhao G (2015a) HARPS observes the Earth transiting the sun – a method to study exoplanet atmospheres using precision spectroscopy on large ground-based telescopes. *The Messenger* 161:17–19
- Yan F, Fosbury RAE, Petr-Gotzens MG, Pallé E, Zhao G (2015b) Using the Rossiter-McLaughlin effect to observe the transmission spectrum of Earth’s atmosphere. *ApJ* 806:L23. <https://doi.org/10.1088/2041-8205/806/2/L23>, 1506.04456
- Yoshikawa I, Ono J, Yoshioka K et al (2008) Observation of Mercury’s sodium exosphere during the transit on November 9, 2006. *Planet Space Sci* 56:1676–1680. <https://doi.org/10.1016/j.pss.2008.07.026>
- Zeng L, Sasselov D (2014) The effect of temperature evolution on the interior structure of H<sub>2</sub>O-rich planets. *ApJ* 784:96. <https://doi.org/10.1088/0004-637X/784/2/96>, 1402.7299